ANNALS of Faculty Engineering Hunedoara – International Journal of Engineering
Tome XX [2022] | Fascicule 3 [August]

1. Janos FERENCZ, 2. Andras KELEMEN, 3. Maria IMECS

PARTICLE SWARM OPTIMIZATION OF AN ELECTRIC VEHICLE HYBRID ENERGY STORAGE SYSTEM

[1] Doctoral School, Faculty of Electrical Engineering, Technical University of Cluj-Napoca, ROMANIA
[2] Department of Electrical Engineering, Faculty of Technical and Human Sciences Târgu Mureş, Sapientia Hungarian University of Transylvania, ROMANIA
[3] Department of Electrical Machines and Drives, Faculty of Electrical Engineering, Technical University of Cluj-Napoca, ROMANIA

Abstract: The paper presents the efficiency optimization of the Hybrid Energy Storage System (HESS) of an Electric Vehicle (EV), composed of a battery and a supercapacitor. The efficiency optimization is carried out by searching the optimal power sharing between the energy storage devices, reducing to a minimum the energy losses. The correct operation of the HESS is subject to several constraints, out of which six have been considered in the optimization problem. The constrained optimization has been performed using the Particle Swarm Optimization (PSO) algorithm, first tested on the Rastrigin function. The implementation of this stochastic optimization method can be a challenge even in low-dimensional cases, due to the non-convex feasible solution space. The paper presents a modified version of the basic PSO algorithm, which can initialize the particle swarm, and find the minimum of the cost function even in very narrow, „needle-like", non-connex domains. The modified PSO algorithm has been tested for the HESS of the EV on a single segment of a standard driving cycle, composed of an acceleration and a braking time interval.
Keywords: Hybrid energy storage system, Electric vehicle, Particle swarm optimization, Constrained optimization

INTRODUCTION

In electric vehicles it is advantageous to solve the electrical energy storage using a combination of high energy density and high power density storage devices. Nowadays such Hybrid Energy Storage Systems (HESS) [9] are built using high energy density Li-ion batteries that provide the high autonomy of the vehicle and high power density [11]. Supercapacitors capable of delivery and absorption of high instantaneous power in case of acceleration and regenerative braking, respectively [3]. The subject of this paper is an active parallel HESS [10], [11] topology shown in Figure 1. The power sharing between the energy storage devices is solved using two bidirectional power electronic converters that make possible the power delivery to the electrical drives in motoring mode and energy storage in regenerative braking mode.

One of the benefits of using such a hybrid storage system is the extension of the life cycle of the battery by relieving its stress during acceleration and braking.

An Energy Management Algorithm (EMA) defines in each moment the power sharing between the battery and the supercapacitor, based on the operation mode, state of the storage devices and other criteria based on the shorter- or longer-term energy management strategy [5]. A model involving these factors is shown in Figure 2 [5].

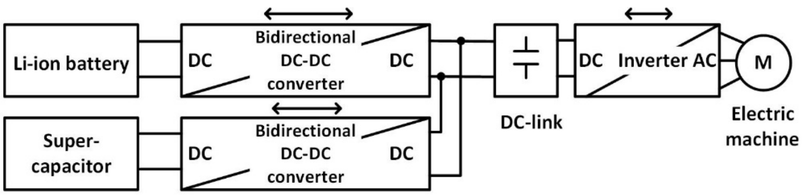

Figure 1: Block diagram of the active parallel hybrid energy storage system (HESS) [5].

The electrical power $\mathbf{p_{el\_req}}$, required in each moment, depends on the instantaneous acceleration and speed ($\mathbf{v}, \mathbf{a}$), defined by the driving cycle, and on the parameters of the vehicle. The power sharing is defined as follows:

$$\begin{cases} p_{SC\_req} = x p_{el\_req} \\ p_{BAT\_req} = (1-x) p_{el\_req}, \end{cases} \tag{1}$$

The abbreviations from Figure 2 represent: the State of Charge of the battery (SOC), the battery current, voltage and internal resistance ($i_{BAT}, u_{BAT}, r_{BAT}$), the State of Energy of the supercapacitor (SOE), and the supercapacitor current, voltage and internal resistance (i_{SC}, u_{SC}, r_{SC}).

This paper deals with the optimization of the energy management algorithm in order to minimize the energy losses in the HESS. In the

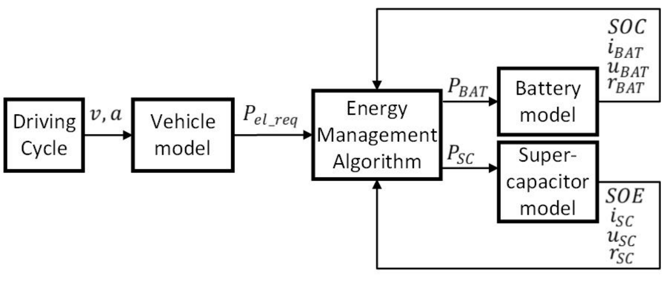

Figure 2: Model including the EMA of the HESS [6].

following chapters the constrained optimization problem is formulated and solved for a simple driving cycle, using a Particle Swarm Optimization (PSO) algorithm [1], [2], [4].

2. THE CONSTRAINED OPTIMIZATION PROBLEM

The overall goal of the presented optimization is the energy loss minimization [14] within the hybrid energy storage system during a standard driving cycle [12], while the optimization variable is the power sharing ratio $x = \frac{p_{SC\_req}}{p_{el\_req}}$.

The optimization problem can be formulated as follows:

Given the system

$$\begin{cases} p_{el_{req}}(t) = f_1\big(a(t), v(t)\big) \\ \frac{du_{BAT}}{dt} = f_2\left(p_{el_{req}}(t), x(t)\right) \\ \frac{dr_{BAT}}{dt} = f_3\left(p_{el_{req}}(t), x(t)\right) \\ \frac{du_{SC}}{dt} = f_4\left(p_{el_{req}}(t), x(t)\right) \end{cases} \quad (2)$$

find $\mathbf{x(t)}$ in order to minimize the objective function

$$W_{loss}(T) = \int_0^T \left(\frac{\left(u_{BAT}(t) - \sqrt{u_{BAT}^2(t) - 4r_{BAT}(t)(1-x(t))p_{el_{req}}(t)}\right)^2}{4r_{BAT}(t)} + \frac{\left(u_{SC}(t) - \sqrt{u_{SC}^2(t) - 4r_{SC}x(t)p_{el_{req}}(t)}\right)^2}{4r_{SC}} \right) dt \quad (3)$$

subject to the bounds on the optimization variable

$$0 \le x(t) \le V \quad (4)$$

and subject to a set of inequality constraints

$$\begin{cases} U_{sc\_MIN} \le u_{sc}(t) \le U_{sc\_MAX} \\ SOC_{MIN} \le SOC(t) \le SOC_{MAX} \\ I_{sc\_MIN} \le i_{sc}(t) \le I_{sc\_MAX} \\ I_{BAT\_MIN} \le i_{BAT}(t) \le I_{BAT\_MAX} \end{cases} \quad (5)$$

The complexity of the problem can be reduced by handling $\mathbf{x(t)}$ as a discrete-time optimization variable with variable discretization period. Thus, the discretization period itself becomes an optimization variable, and the optimization vector is the vector of the sampled power sharing ratio, extended with the vector of the sampling instants:

$$\mathbf{x}_m^* = [\mathbf{x}_m, \boldsymbol{\tau}_m] = [x_1, x_2, \ldots x_P, \tau_1, \tau_2, \ldots \tau_{P-1}] = \arg\min_{\mathbf{x}^*}\left(W_{loss}^{\langle N \rangle}\right). \quad (6)$$

In the vector defined by (6), $\tau_i = \frac{t_i}{T}$ are the sampling instants normalized to the driving cycle period, thus $\tau_i \in [0,1],\ \text{where } i \in \{1 \ldots N\}$. The optimization vector is subject to the additional bounds:

$$\tau_i < \tau_{i+1}. \quad (7)$$

3. APPLICATION OF THE PARTICLE SWARM OPTIMIZATION ALGORITHM TO THE HESS

In the paper the Particle Swarm Optimization (PSO) algorithm has been used to solve a constrained optimization problem for a reduced dimension of the optimization vector.

After the initial placement („initialization") of the elements of a particle swarm, this stochastic algorithm attempts to move the particles towards the global optimum based on the individual and collective results of the cost function evaluation.

The task of the initialization process is to drop the particles of a swarm in valid positions delimited by the constraints. In comparison with [6], where a single constraint has been applied, the introduction of the eight constraints according to (5) results in very narrow, needle-like domains of validity for the optimization vector. This fact increases drastically the execution time of the initialization process of the PSO algorithm, and hence the need for a modified initialization algorithm, able to create efficiently an initial population even in such narrow domains of validity.

During the subsequent optimization phase of the algorithm, the positions of the particles are recalculated according to [2], [8], [13]:

$$\begin{cases} \mathbf{v}_i^{k+1} = \omega \mathbf{v}_i^k + c_1 \mathbf{rand}_{i1}^k \odot \left(\mathbf{r}_{Bi}^k - \mathbf{r}_i^k\right) + c_2 \mathbf{rand}_{i2}^k \odot \left(\mathbf{r}_G^k - \mathbf{r}_i^k\right) \\ \mathbf{r}_i^{k+1} = \mathbf{r}_i^k + \mathbf{v}_i^{k+1} \end{cases}, \quad (8)$$

where the notations stand for:

$\mathbf{r}_i^k$ – position vector of particle i in the k-th step of the search;

$\mathbf{v}_i^k$ – „speed" of particle i in the k-th step of the search;
$\mathbf{r}_{Bi}^k$ – individual best position vector of particle i until the k-th step of the search;
$\mathbf{r}_G^k$ – best position vector of any particle from the swarm until the k-th step of the search;
$\mathbf{rand}_{i1}^k$ and $\mathbf{rand}_{i2}^k$ are random vectors, with elements with continuous uniform distribution, in the range $[0,1]$;
ω – inertia weight;
c_1 – cognitive learning factor;
c_2 – social learning factor;
$\odot$ – Hadamard product of vectors.

Different behaviours, such as the "absorbing" and "invisible" one, have been defined for handling the particle motion in the presence of constraints [7]. In [6] it has been introduced a "halving" method, which is applied in this paper as well.

This behaviour is illustrated in Figure 3, in case of a two-dimensional search space. If the displacement generated by (5) crosses a constraint boundary, the direction is preserved, but the size of the step is halved until the particle gets back to the domain of validity. In this case, the positions $r_i^{k+1}|_{\text{trial 1}}$ and $r_i^{k+1}|_{\text{trial 2}}$ are outside of the domain of validity, thus the distance between r_i^{k+1} and r_i^k is halved until reaching $r_i^{k+1}|_{\text{trial 3}}$.

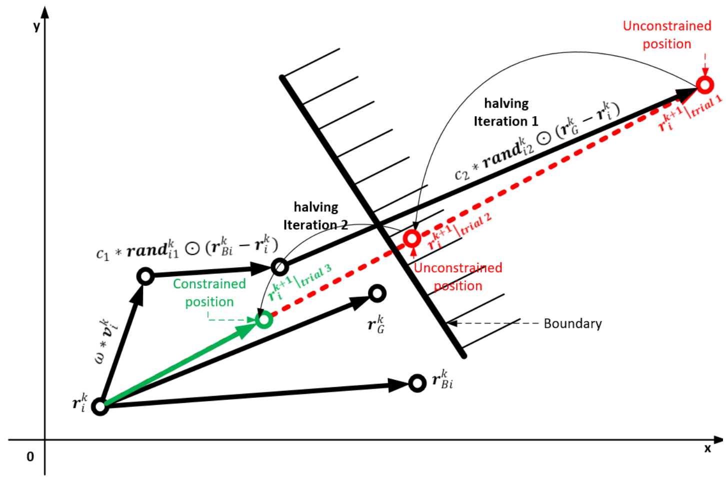

Figure 3: The constrained particle swarm optimization algorithm in a two-dimensional space, with „halving" behaviour

4. INITIALIZATION OF THE CONSTRAINED PSO ALGORITHM FOR THE HESS

Generally, the initial position of the swarm is determined by random placement of the particles in the domain delimited by the constraints. In case of the HESS optimization, it is difficult or impossible to find an analytical form of the multidimensional constraints. Thus, the validation of the generated position of a particle becomes a matter of trial and error. If any of the constraints proves to be active, the particle is thrown away and the process is repeated until the successful placement of a population with sufficient particles in order to start the search for optimum.

In case of the presence of multiple constraints it can be observed, that the search for the optimal solution has to be performed within very narrow, „needle-like" domains, for which the above initialization method is extremely slow. Moreover, as the probability of placing particles in such needle-like domains is very reduced, it can happen that optimal solutions within these domains are never found, because the large number of particles placed in less narrow domains tend to prevail in the PSO search process.

The modified initialization algorithm proposed in the paper is composed of two main steps. First, new points are randomly generated within the search space until a valid point is found in the close neighbourhood of a constraint boundary, and the directions of the neighbouring boundaries are determined for this point.

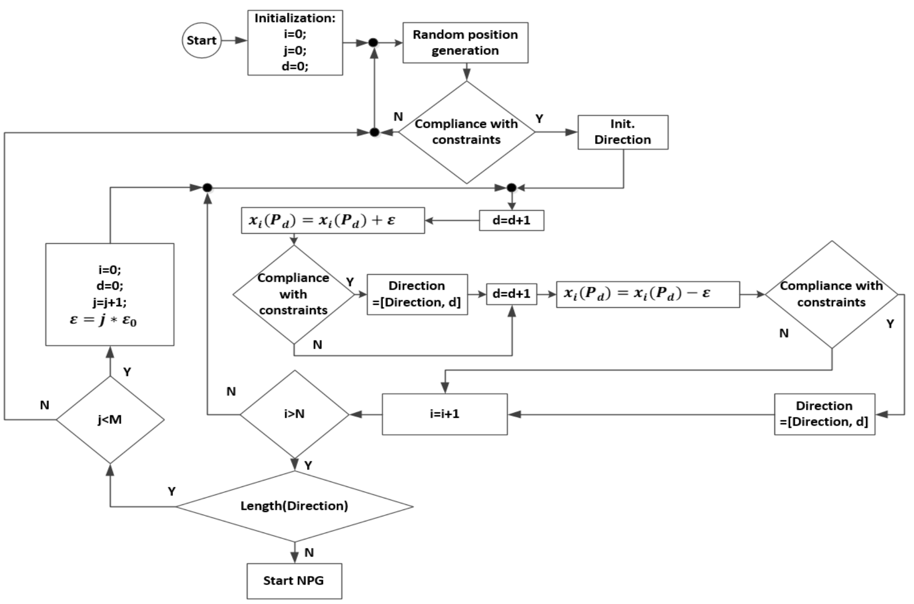

Figure 4: Flowchart of the NPG initialization algorithm in an N-dimensional search space

In the second step, new particles are generated in these directions in order to boost the number of particles that penetrate into narrow gaps along the boundaries. This process is referred to as New Point Generation (NPG).

As shown in Figure 4 for an N-dimensional search space, the above "neighbourhood" is defined by a radius initialized with ε in each of the $2N$ main directions of the search space, and it is step-by-step increased up to m times by a multiple of the initial radius, until at least two boundaries are hit.

If the point obtained in this way is not in the neighbourhood of at least two constraint boundaries, the particle is still included in the initial swarm, but the NPG process is stopped, and the next particle is obtained by random generation as explained above.

In Figure 5 the same algorithm is graphically illustrated for a two-dimensional search space. The constrained domain is limited by two sharp-angled lines

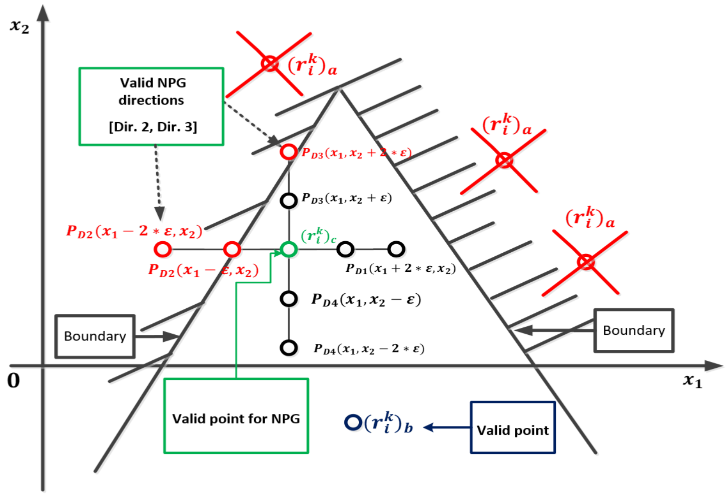

Figure 5: Detection of the direction of the constraint in a two-dimensional space.

The particles pointed at by $(\mathbf{r}_i^k)_a$, (referred to as type "a") are not valid, being outside the constrained domain. The particles pointed at by $(\mathbf{r}_i^k)_b$, (referred to as type "b") are included in the swarm, but they are not used for new point generation, being placed in a "free" area, far away from the boundaries. The particles pointed at by $(\mathbf{r}_i^k)_c$, (referred to as type "c") are used by the NPG algorithm to generate new points along the boundaries. In this two-dimensional case, four main directions are defined to be used by the NPG, and the initial radius ε had to be doubled in order to validate the position.

The flow chart of the NPG algorithm is shown in Figure 6. Generation of new particle positions starting from the points type "c" is preferentially attempted in the directions of the closest boundaries.

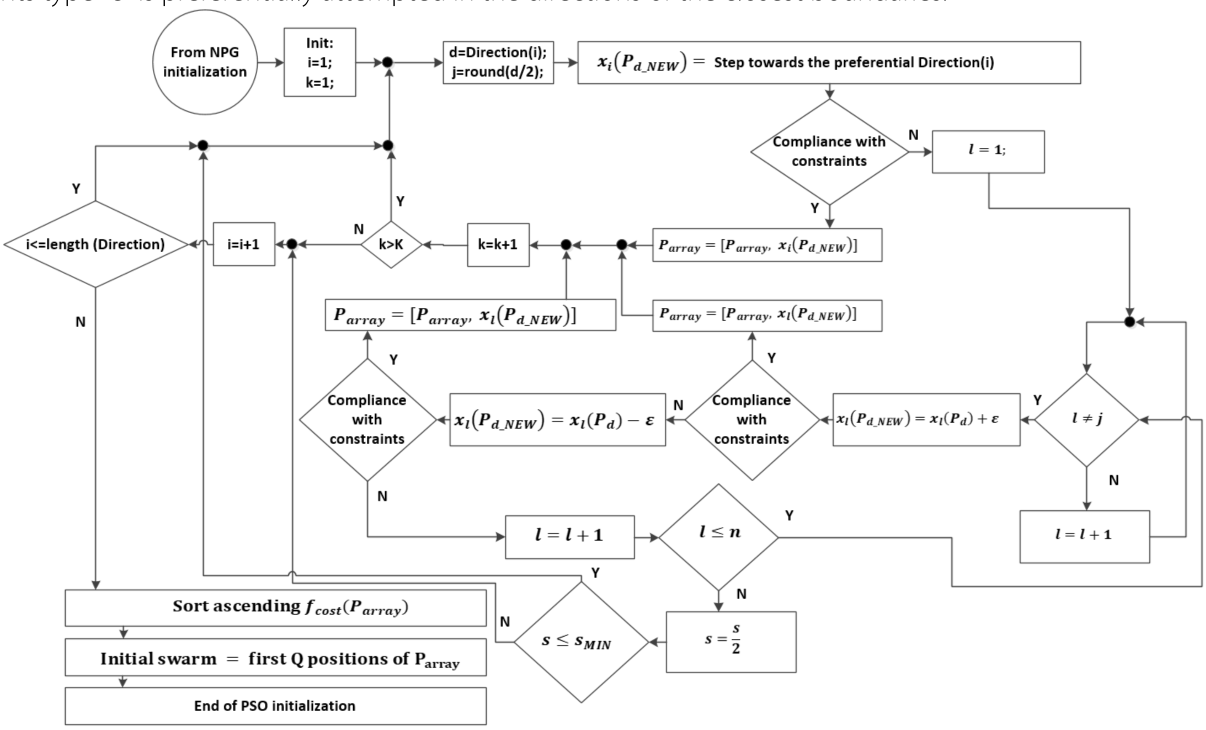

Figure 6: Flowchart of the algorithm for generation of new points that comply with the constraints in an N- dimensional search space.

This means that a first step sized "s" is made in one of these directions, and the position is accepted if it complies with the constraints. Otherwise, the same trial is made in the other possible directions, except backwards. In case of unsuccessful trials, the step is decreased until reaching an s_{MIN} limit, which means the arrival to the „tip of the needle". Each new valid position becomes the host of a new particle, and the new starting point for the above process, in which the first trial is always made in the preferential direction that confines the NPG to a trajectory in the neighbourhood of the boundaries Advancement towards the "open space" is also limited by limiting the number of steps to "k".

After the NPG towards each preferential direction is finished, the objective function is evaluated for each position, and the best ones are used to initialize the swarm for the PSO search algorithm.

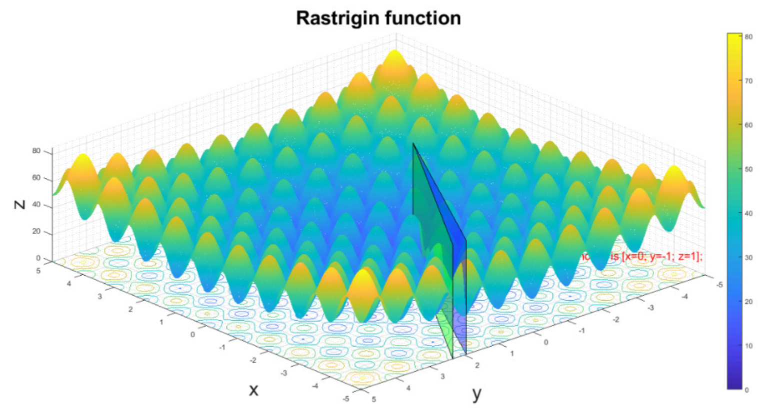

Figure 7: The Rastrigin function used for the performance test of the constrained optimization algorithm. The constraints have been defined so that the boundary includes the global minimum.

The presented initialization algorithm is much faster than the one based exclusively on the random particle placement, and it results in an initial positioning that is already close to the minima of the constrained domain.

The initialization algorithm has been tested on the two-dimensional Rastrigin function, using constraints defined as two planes that form a sharp angle of about 4°, according to Figure 7.

The tests have been performed using a computer with Intel I7 processor, 8 GB RAM DDR3, and 256 GB SSD.

During this test, in order to generate a swarm of 25 particles, the radius for the detection of the valid directions was $\varepsilon = 0.05$, the initial step of $s = 0.1$ was possibly halved down to $s_{MIN} = 0.0001$, while the maximum number of iterations was $K = 400$.

During the first step of the initialization algorithm, there resulted several invalid points, and only three points that comply with the constraints (shown in Figure 8).

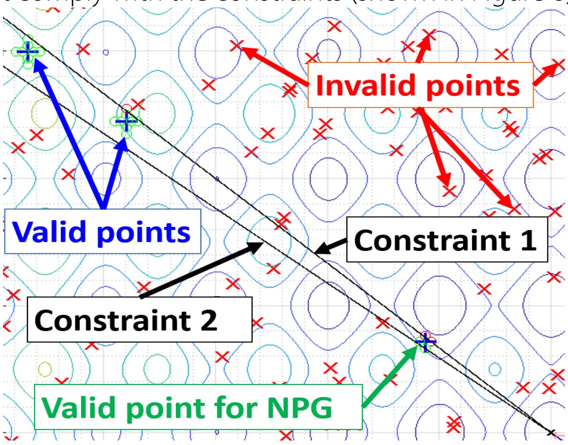

Figure 8: Detection of the direction of the closest constraint boundaries, and definition of a starting point for NPG.

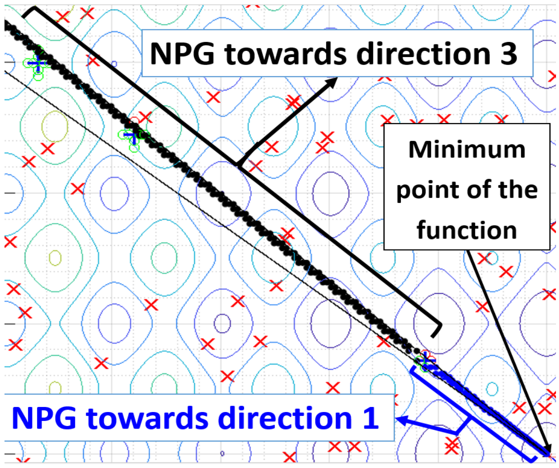

Figure 9: NPG towards two preferential directions.

Out of these, only one is valid for NPG, i.e. lies in two directions closer than $\varepsilon = 0.05$ to constraint boundaries. In the second step of the initialization algorithm, new particle positions have been generated in the preferential directions, according to the NPG algorithm, out of which a number of 25 with the lowest value of the corresponding cost function, have been chosen as the initial position of the swarm (shown in Figure 9).

Both the basic and the modified initialization algorithms have been executed 20 times.

The statistics from Figure 10 show that in this test the modified algorithm proved to be about 19 times faster, than the basic initialization.

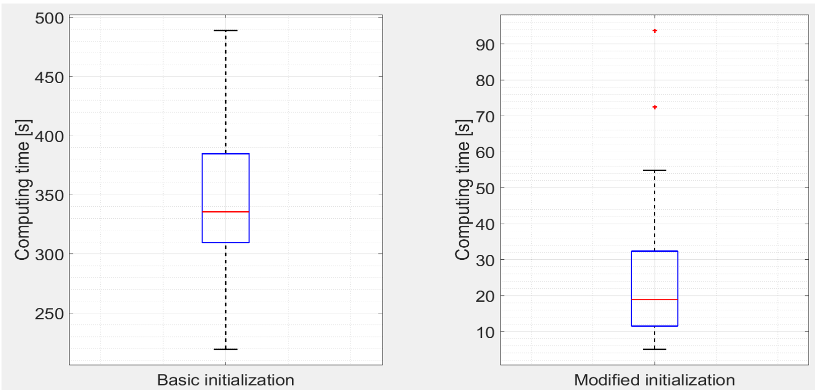

Figure 10: Boxplot statistics of the computing time for the initialization shown in Figure 9.

5. PARTICLE SWARM MINIMIZATION OF THE HESS ENERGY LOSSES

The active parallel HESS presented in Figure 1, with the parameters from Table 1, has been used as the power supply for an $m = 1611$ kg vehicle during a driving cycle shown in Figure 11.

Table 1: The parameters of the HESS, used for simulation.

Battery	Capacity	Q_{wh}	1000 Wh
	No load voltage	u_{BAT}	800 V
	Initial state of charge	SOC_{init}	100 %
	Internal resistance at SOC=100%	$r_{BAT}\|_{SOC=100\%}$	300 mΩ
	Internal resistance at SOC=50%	$r_{BAT}\|_{SOC=50\%}$	650 mΩ
Supercapacitor	Capacity	C_{SC}	10 F
	Initial voltage	U_{SC_init}	800 V
	Internal resistance	r_{SC}	100 mΩ
Restrictions	Maximum supercapacitor voltage	U_{sc_MAX}	800 V
	Minimum supercapacitor voltage	U_{sc_MIN}	700 V
	Maximum SOC value	SOC_{MAX}	100 %
	Minimum SOC value	SOC_{MIN}	64 %
	Maximum supercapacitor current	I_{sc_MAX}	100 A
	Minimum supercapacitor current	I_{sc_MIN}	-100 A
	Minimum battery current	I_{BAT_MAX}	40 A
	Maximum battery current	I_{BAT_MIN}	-45 A

In Figure 12 the contour map of the objective function (3) is represented for a two-element search vector $[x_1, x_2]$, and a fixed division of the driving cycle period at $\tau_1 = 50$ s.

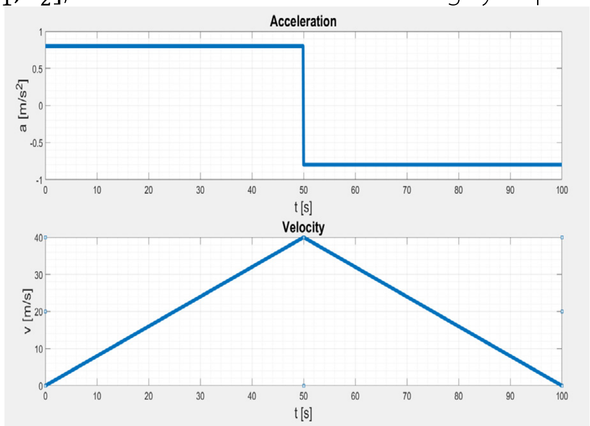

Figure 11: The simple driving cycle used to demonstrate the modified initialization algorithm of the PSO in case of the constrained energy loss optimization of the HESS.

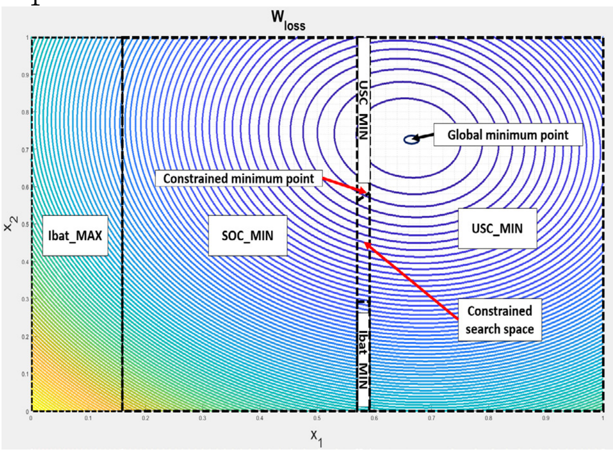

Figure 12: Contour map of the total energy loss during the driving cycle. Six constraints are active in different regions of the search space.

In this case, six of the eight constraints from (5) are active in different regions of the search space, and the region that complies with the constraints is only a narrow strip.

Figure 13 shows the points randomly generated in the first phase of the initialization, while Figure 14 shows the new points generated in the preferential directions.

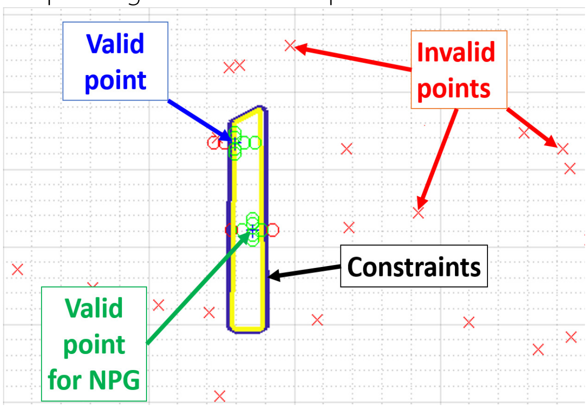

Figure 13: Detection of the constraint boundary directions, and definition of a starting point for NPG.

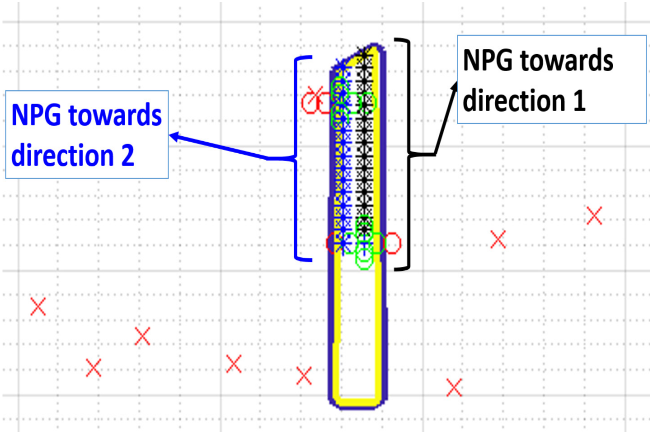

Figure 14: NPG towards two preferential directions

Both the basic and the modified initialization algorithms have been executed 20 times to create the boxplot statistics of the computing time, shown in Figure 15., which shows that the modified algorithm is almost 20 times faster.

Further tests have been made regarding the execution time of the whole PSO algorithm for the same conditions, using two versions of the dynamic division of the driving cycle [6], which yield $\mathbf{x}_m^* = [x_1, x_2, \tau_1]$ and $\mathbf{x}_m^* = [x_1, x_2, x_3, \tau_1, \tau_2]$, respectively.

Both versions have been executed 10 times for each algorithm, and the statistics of the execution times are shown in Figure 16 and Figure 17.

The total execution time using the modified initialization algorithm is 12.5 times shorter in the 3-dimensional case, and 2.5 times shorter in the 5-dimensional case, than using the basic initialization.

Figure 18 shows the evolution in time of the state variables of the HESS using the results of the 5-dimensional optimization. It can be noticed that the variables are kept within the boundaries defined by the constraints.

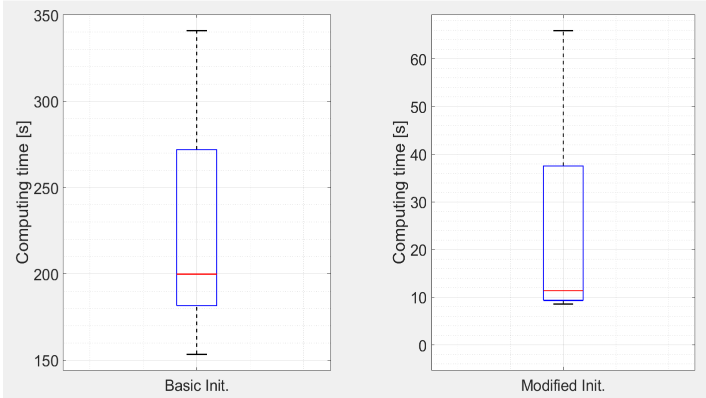

Figure 15: Boxplot statistics of the computing time of the Basic PSO initialization and of the modified initialization algorithm

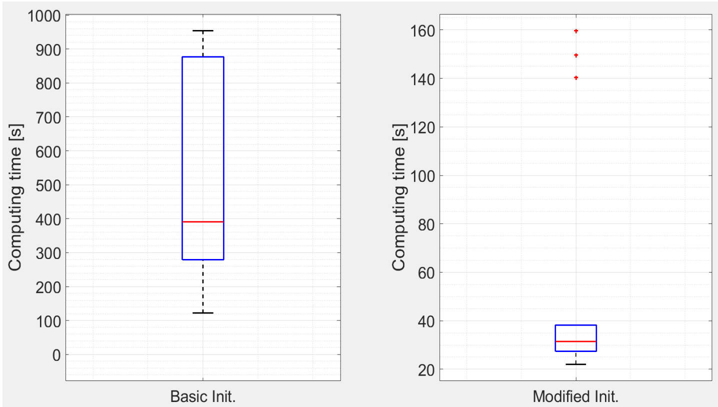

Figure 16: Boxplot statistics of the total PSO computing time for the basic and for the modified initialization algorithm in the case of a 3-dimensional search space.

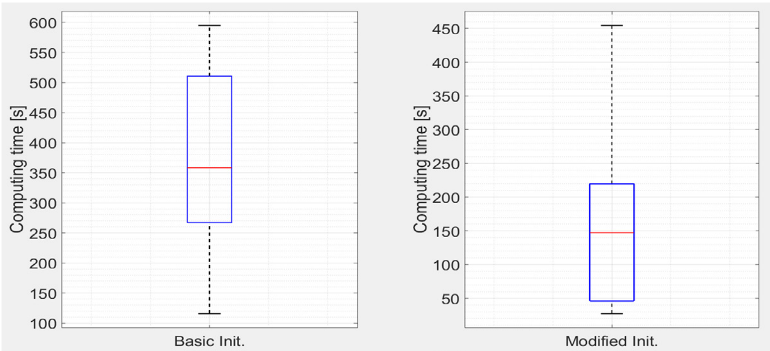

Figure 17: Boxplot statistics of the total PSO computing time for the basic and for the modified initialization algorithm in the case of a 5-dimensional search space.

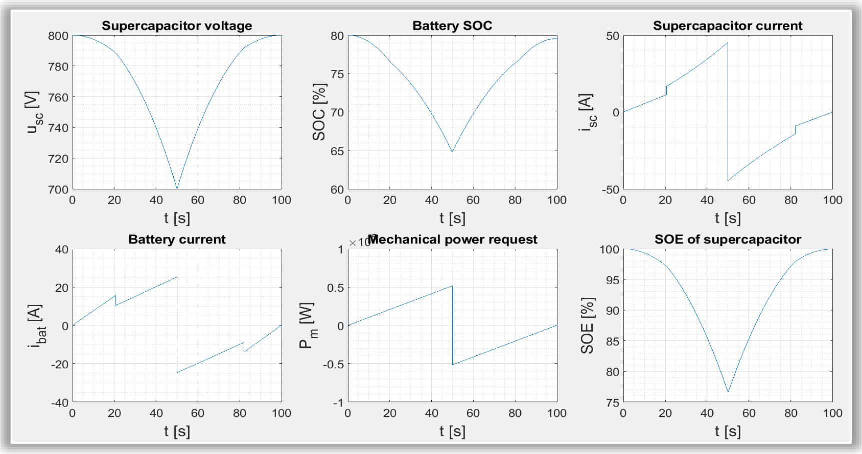

Figure 18: Time diagrams of the HESS state variables in case of $\mathbf{x}^* = \mathbf{x}_m^*$.

6. CONCLUSIONS

The PSO initialization algorithm introduced in this paper ensures a much faster execution of the initialization, than the previously used random placement of the particles. This advantage becomes evident in case of the constrained optimization problem of a hybrid energy storage system, where the placement and movement of the particles is confined by the multiple constraints to very narrow subdomains. Finding the optimal solution in hardly accessible areas is made possible, and the efficiency of the whole particle swarm optimization algorithm is significantly increased.

Note: This paper was presented at CNAE 2022 – XXth National Conference of Electric Drives, organized by University POLITEHNICA Timisoara, Faculty of Faculty of Electrotechnics and Electroenergetics (ROMANIA), in Timisoara, ROMANIA, in 12-13 May, 2022

References

[1] Ammari C; Belatrache D; Touhami B; and Makhlouf S: Sizing, Optimization, Control and Energy Management of Hybrid Renewable Energy System — A Review, KeAi. Energy and Built Environment, vol. 2, pp. 23-53, 2021.
[2] Borgulya I: Optimalizálás Evolúciós Számításokkal, Budapest, Typotex, 2011.
[3] Capassoa C; Lauria D; and Veneria O: Optimal Control Strategy of Ultra-Capacitors in Hybrid Energy Storage System for Electric Vehicles, Elsevier, Energy Procedia, vol. 142, pp. 1914-1919, 2017.
[4] Chong LW; Wong YW; and Rajkumar RK: An Optimal Control Strategy for Standalone PV System with Battery Supercapacitor Hybrid Energy Storage System, Elsevier. Journal of Power Sources, vol. 331, pp. 553-565, 2016.
[5] Ferencz J; Kelemen A; and Imecs, M: Control of an Electric Vehicle Hybrid Energy Storage System, Sciendo, Papers on Technical Science, vol. 14, pp. 77-88, 2021.
[6] Ferencz J; Kelemen A; and Imecs M: Particle Swarm Optimization of a Hybrid Energy Storage System, Acta Universitatis Sapientiae Electrical and Mechanical Engineering, vol. 13, pp. 82-100, 2021.
[7] Huang T, and Mohan AS: A Hybrid Boundary Condition for Robust Particle Swarm Optimization, IEEE Antennas and Wireless Propagation Letters, vol. 4, pp. 112-117, 2005.
[8] Kanglong Y; Peiqing L; and Hao L: Optimization of Hybrid Energy Storage System Control Strategy for Pure Electric Vehicle Based On Typical Driving Cycle, Hindawi. Mathematical Problems in Engineering, vol. 2020, pp. 1-12, 2020.
[9] Paul T; Mesbahi T; and Durand S: Sizing of Lithium-Ion Battery/Supercapacitor Hybrid Energy Storage System for Forklift Vehicle, Energies, vol. 13, pp. 1-18, 2020.
[10] Romaus C; Gathmann K; and Böcker J: Optimal energy management for a hybrid energy storage system for electric vehicles based on stochastic dynamic programming, Vehicle Power and Propulsion Conference, pp. 1-6, 2010.
[11] Sadeq T; Wai CK; Morris E; Tarbosh QA; and Aydoğdu Ö: Optimal Control Strategy to Maximize the Performance of Hybrid Energy Storage System for Electric Vehicle Considering Topography Information, IEEE Access, vol. 8, pp. 1-13, 2020.
[12] Vinot E; and Trigui R: Optimal Energy Management of HEVs with Hybrid Storage System, HAL open science. Energy Conversion and Management, vol. 76, pp. 437-452, 2019.
[13] Wang D; Tan D; and Liu L: Particle Swarm Optimization Algorithm: An Overview, Springer Link. Soft Computing, vol. 22, pp. 387-408, 2017.
Ye K; and Li P: A New Adaptive PSO-PID Control Strategy of Hybrid Energy Storage System for Electric Vehicles, Sage. Advances in Mechanical Engineering, vol. 12, pp. 1-15, 2020.

ISSN 1584 – 2665 (printed version); ISSN 2601 – 2332 (online); ISSN-L 1584 – 2665